

# Synthesis of Cyclopentadienyl-Based Trioxo-rhenium Complexes and Their Use as Deoxydehydration Catalysts

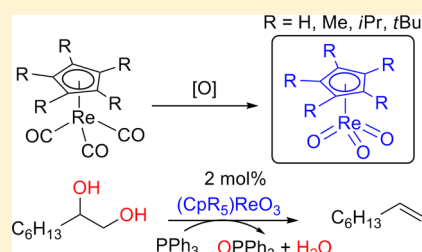
Suresh Raju,<sup>†</sup> Christian A. M. R. van Slagmaat,<sup>†</sup> Jing Li,<sup>†</sup> Martin Lutz,<sup>‡</sup> Johann T. B. H. Jastrzebski,<sup>†</sup> Marc-Etienne Moret,<sup>†</sup> and Robertus J. M. Klein Gebbink<sup>\*,†</sup>

<sup>†</sup>Organic Chemistry and Catalysis, Debye Institute for Nanomaterials Science, Faculty of Science, Utrecht University, Universiteitsweg 99, Utrecht 3584 CG, The Netherlands

<sup>‡</sup>Crystal and Structural Chemistry, Bijvoet Center for Biomolecular Research, Faculty of Science, Utrecht University, Padualaan 8, Utrecht 3584 CH, The Netherlands

## S Supporting Information

**ABSTRACT:** The cyclopentadienyl-based trioxo-rhenium complexes  $\text{Cp}^{\text{ttt}}\text{ReO}_3$  ( $\text{Cp}^{\text{ttt}}$  = 1,2,4-tritert-butylcyclopentadienyl) **1b** and  $\text{Cp}^*\text{ReO}_3$  ( $\text{Cp}^*$  = pentamethylcyclopentadienyl) **4b**) are known to be active catalysts for the deoxydehydration (DODH) of vicinal diols to olefins. Here, we report on the preparation of a series of complexes of the general formula  $\text{Cp}'\text{ReO}_3$  ( $\text{Cp}'$  = 1,3-di-*tert*-butylcyclopentadienyl ( $\text{Cp}^{\text{t}}$ , **2b**, 18%), 1,2,3-triisopropylcyclopentadienyl (**3b**, 4%), 1,2,3-trimethyl-4,5,6,7-tetrahydroindenyl (**6b**, 36%), and tetramethylcyclopentadienyl (**7b**, 33%)) in which the electronic and steric properties of the  $\text{Cp}'$  ligand are varied. These complexes were synthesized via oxidative decarbonylation from the corresponding  $\text{Cp}'\text{Re}(\text{CO})_3$  complexes with either  $\text{H}_2\text{O}_2$  or *t*BuOOH. An *in situ* NMR investigation revealed that complexes **2b**, **3b**, and **6b** are unstable under the oxidizing reaction conditions. This information was used to determine the optimal reaction time to isolate the complexes **2b**, **3b**, and **6b**. These “piano-stool” configured  $\text{Cp}'\text{ReO}_3$  complexes were characterized spectroscopically and by single crystal X-ray diffraction. The new complexes **2b**, **3b**, **6b**, and **7b** were found to be generally less thermally stable than  $\text{Cp}^{\text{ttt}}\text{ReO}_3$  (**1b**) or  $\text{Cp}^*\text{ReO}_3$  (**4b**). It appeared that **2b** and **6b** were better catalysts for the DODH of 1,2-octanediol to octene with  $\text{PPh}_3$  as an oxygen-atom acceptor. Remarkably, the less substituted  $\text{Cp}'\text{ReO}_3$  complexes (**1b**, **2b**, and **3b**) afforded significantly less 2-octene (presumably from isomerization of the primary 1-octene product) in comparison to those containing per-alkylated Cp-moieties (**4b** and **6b**).



## INTRODUCTION

Sustainable industrial production of chemicals will benefit from new synthetic routes starting from renewable feedstocks such as biomass-derived polysaccharides and sugar and polyol derivatives. Unlike the currently used fossil hydrocarbons, these new starting materials are overfunctionalized with oxygen atoms.<sup>1–4</sup> Hence, there is a renewed interest in catalytic deoxygenation methods, and especially in deoxydehydration (DODH) reactions that convert vicinal diols to olefins.<sup>5–7</sup> The best catalysts for these reactions are currently rhenium-based; in particular, methyltrioxorhenium (MTO) has been shown to be a versatile DODH catalyst in combination with a range of external reductants.<sup>8–11</sup> The simple methyl substitution that keeps the high Lewis acidity of the rhenium center is thought to facilitate the coordination of substrate molecules. However, derivatives of MTO containing longer chain alkyl groups are unstable even at low temperatures, preventing systematic variations for further catalyst development.<sup>12–14</sup>

However, the cyclopentadienyl-based trioxo-rhenium catalyst  $\text{Cp}^*\text{ReO}_3$  ( $\text{Cp}^*$  = 1,2,3,4,5-pentamethylcyclopentadienyl) is long known to catalyze DODH reactions of vicinal diols including bioderived polyols.<sup>15</sup> However, this system suffers from some major drawbacks such as low (<55) catalytic turnover number (TON), the requirement of a strong and

expensive stoichiometric reductant ( $\text{PPh}_3$ ), and rapid catalyst decomposition to multinuclear clusteric oxo-rhenium species.<sup>15,16</sup> These issues were partly overcome by introducing a bulky 1,2,4-tritert-butylcyclopentadienyl ( $\text{Cp}^{\text{ttt}}$ ) ligand:  $\text{Cp}^{\text{ttt}}\text{ReO}_3$  displays better TONs (up to 1400) and is able to perform DODH with other reductants such as *sec.* alcohols and hydrogen.<sup>17a,b</sup> Hence, systematic variations of multiply substituted Cp-based trioxo-rhenium catalysts are desirable for further optimization.

At the beginning of this work, only a limited number of other Cp-based trioxo-rhenium complexes were known in the literature:  $\text{CpReO}_3$ ,<sup>18–20</sup>  $(\text{CpMe})\text{ReO}_3$ ,<sup>19</sup> and  $(\text{CpEtMe}_4)\text{ReO}_3$ .<sup>21</sup> This is likely due to the synthetic difficulties encountered when preparing these high-valent  $\text{Re}(\text{VII})$  trioxo complexes. Two methods were reported for the preparation of  $\text{Cp}'\text{ReO}_3$  complexes depending on the redox potential of the  $\text{Cp}'$  ligands ( $\text{Cp}'$  = substituted cyclopentadienyl; substituted indenyls are also abbreviated as  $\text{Cp}'$  for simplicity).<sup>22</sup> For electron-poor ligands, the method of choice is the transmetalation reaction of  $\text{XReO}_3$  ( $\text{X}^- = \text{ReO}_4^-$ ,  $\text{Cl}^-$ , and  $\text{CF}_3\text{COO}^-$ ) with  $\text{Cp}'_2\text{Zn}$  or  $\text{Bu}_3\text{Cp}'\text{Sn}$  to obtain  $\text{Cp}'\text{ReO}_3$ .

Received: February 12, 2016

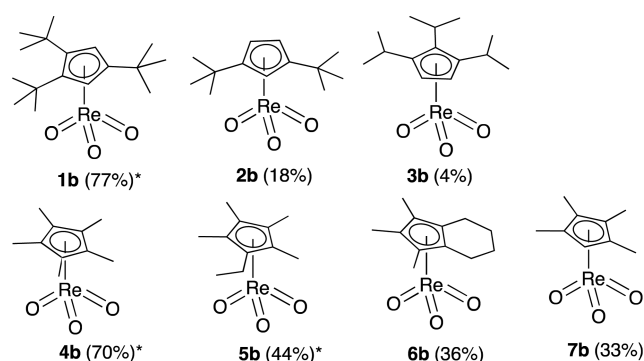
Published: June 16, 2016



(Cp' = Cp<sup>18–20</sup> or CpMe<sup>19</sup>). In contrast, highly substituted, electron-rich Cp'ReO<sub>3</sub> (Cp' = Cp\*,<sup>23–25</sup> CpEtMe<sub>4</sub>,<sup>21</sup> or Cp<sup>ttt17</sup>) complexes can be obtained by oxidative decarbonylation of Cp'Re(CO)<sub>3</sub> with H<sub>2</sub>O<sub>2</sub> as oxidant.<sup>26</sup> In addition, oxidative decarbonylation for the formation of Cp\*ReO<sub>3</sub> was demonstrated with other oxidants such as O<sub>2</sub>,<sup>27,28</sup> O<sub>3</sub>,<sup>29</sup> Mn<sub>2</sub>O<sub>7</sub>,<sup>30</sup> *t*BuOOH,<sup>31</sup> and dimethyldioxirane.<sup>32</sup> These electron-rich Cp'ReO<sub>3</sub> complexes display improved thermal stability compared to that of electron-poor Cp'ReO<sub>3</sub> complexes. The decomposition temperature was determined by thermogravimetric analysis: Cp, 134.2 °C; CpMe, 144.7 °C; Cp\*, 207.8 °C; and CpEtMe<sub>4</sub>, 166.0 °C.<sup>13,22,31,33</sup>

Here, we report the preparation of a series of alkyl-substituted Cp'ReO<sub>3</sub> complexes (**1b–7b**, Chart 1) by oxidative

Chart 1. Cp'ReO<sub>3</sub> Complexes **1b–7b** (Including Isolated Yields)



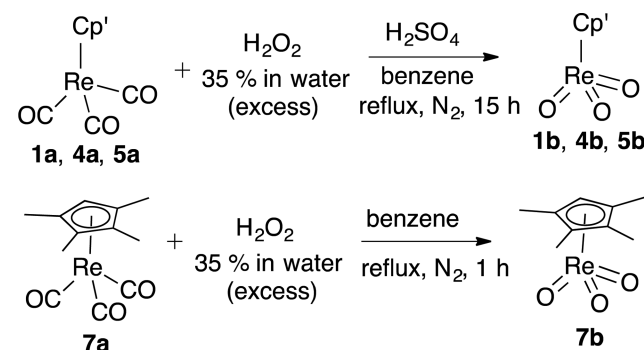
\* Literature values.

decarbonylation of the corresponding tricarbonyl complexes (**1a–7a**). *t*BuOOH is identified as the oxidant of choice for sensitive complexes that decompose under oxidative conditions, and we report an NMR method to determine the optimal conditions and reaction time in these cases. Under the same conditions, the desired Cp'ReO<sub>3</sub> complexes were not observed for aryl-substituted Cp'H ligands CpPh<sub>5</sub>H (1,2,3,4,5-pentaphenylcyclopentadiene), CpPh<sub>4</sub>H<sub>2</sub> (1,2,3,4-tetraphenylcyclopentadiene), or IndPh<sub>3</sub>H (1,2,3-triphenylindene). The catalytic activity of complexes **1b–7b** in the DODH of 1,2-octanediol to 1-octene with PPh<sub>3</sub> as reductant is compared to investigate structure–activity relationships.

## RESULTS AND DISCUSSION

**Synthesis of Trioxo-rhenium Complexes.** The alkyl-substituted Cp'Re(CO)<sub>3</sub> complexes **1a–7a** (**3a** and **3a'** is 1,2,3- and 1,2,4-Cp-substituted (Cp*i*Pr<sub>3</sub>H<sub>2</sub>)Re(CO)<sub>3</sub>, respectively) can be prepared under neat reaction conditions by reacting the corresponding Cp'H ligands with Re<sub>2</sub>(CO)<sub>10</sub>, while aryl-substituted complexes are obtained by the reaction of LiCp' (Cp' = CpPh<sub>5</sub>, CpPh<sub>4</sub>H, IndPh<sub>3</sub>) with BrRe(CO)<sub>5</sub>.<sup>17c</sup> The known rhenium trioxo complexes **1b**, **4b**, and **5b** were synthesized by decarbonylative oxidation of the corresponding rhenium tricarbonyl complexes (**1a**, **4a**, and **5a**) according to literature procedures (Scheme 1).<sup>17,23</sup> A biphasic oxidation reaction was performed by using an excess (20–30 equiv) of H<sub>2</sub>O<sub>2</sub> (35% in water) with a catalytic amount of conc. H<sub>2</sub>SO<sub>4</sub> in benzene at 80 °C for 15 h. After the reaction, the mixture was extracted with benzene, and the organic phase was washed with water, 5% aqueous NaHCO<sub>3</sub>, and brine. Then, solvent

Scheme 1. Synthesis of Alkyl-Substituted Cp'ReO<sub>3</sub> Complexes by Oxidative Decarbonylation of Cp'Re(CO)<sub>3</sub> Complexes by Using H<sub>2</sub>O<sub>2</sub> Solution



evaporation *in vacuo* afforded bright yellow crystals of **1b**, **4b**, and **5b**.

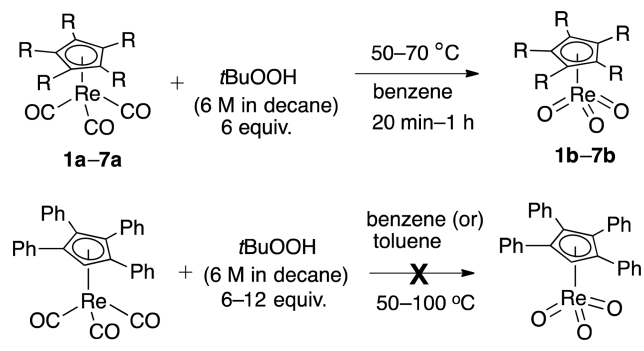
In contrast, when **2a**, **6a**, (**3a** + **3a'**), and **7a** were subjected to these reaction conditions, a yellow-brown oily mixture was obtained. According to thin layer chromatography (TLC) and NMR, it was found not to contain the starting Cp'Re(CO)<sub>3</sub> complexes (**2a**, **6a**, (**3a** + **3a'**), and **7a**) or the expected Cp'ReO<sub>3</sub> complexes (**1b**, **6b**, (**3b** + **3b'**), and **7b**). The synthesis attempts for the phenyl-substituted complexes Cp'ReO<sub>3</sub> (Cp' = CpPh<sub>5</sub>, CpPh<sub>4</sub>H, IndPh<sub>3</sub>) using H<sub>2</sub>O<sub>2</sub> biphasic conditions were also not successful. The starting complex **7a** was further tested under varying biphasic reaction conditions. Excluding catalytic H<sub>2</sub>SO<sub>4</sub> under prolonged reflux reactions also resulted in an intractable mixture of products. However, the appearance of the yellow color typical of Cp-ligated trioxo-rhenium complexes at early reaction times prompted us to stop the reaction after a short reaction time (1 h), which allowed for the isolation of **7b** as a yellow solid in 33% (Scheme 1).

Attempts to synthesize **2b** under similar biphasic conditions with H<sub>2</sub>O<sub>2</sub> as the oxidant were unsuccessful. Thus, we turned to the methodology developed by Kochi for Cp\*ReO<sub>3</sub> (31–36% maximum yield), which involves homogeneous oxidation of Cp\*Re(CO)<sub>3</sub> by *t*BuOOH (purified by distillation) over short reaction times (5–10 min) at 80 °C.<sup>31</sup> In our case, a commercially available *t*BuOOH solution (6 M in decane) was used instead. After the addition of *t*BuOOH, a solution of **2a** in benzene remained colorless for 45 min at room temperature. It was then placed in an oil bath at 85 °C, resulting in a color change to yellow over 10–15 min followed by dark-brown after 20 min, at which point the reaction was stopped by cooling the mixture in an ice bath. The dark-brown oily mixture obtained after solvent evaporation did not contain the desired trioxo-rhenium species. However, the initial appearance of a light yellow color suggested that the desired product might be formed transiently.

The homogeneous character of the latter reactions rendered them amenable to *in situ* monitoring by NMR, which allowed one (1) to determine whether the desired products are formed at all and (2) to determine optimal conditions (reaction time and temperature) for a series of substituted Cp-ligands. Thus, complexes **1a–7a** were subjected to the following experiment: To a solution of the Cp'Re(CO)<sub>3</sub> complex in C<sub>6</sub>D<sub>6</sub> (ca. 40 mM) a stoichiometric amount of *t*BuOOH (6 equiv) was added. There was no visible reaction at RT, and the reaction mixtures were heated gradually from RT inside the NMR

spectrometer until the conversion of tricarbonyl rhenium complex started (Scheme 2). The reaction was monitored at that temperature until no more conversion of the starting  $\text{Cp}^*\text{Re}(\text{CO})_3$  complex was observed.

**Scheme 2. Oxidative Decarbonylation of  $\text{Cp}^*\text{Re}(\text{CO})_3$  Complexes to  $\text{Cp}^*\text{ReO}_3$  Complexes Using  $t\text{BuOOH}$**



In most cases, the formation of  $\text{Cp}^*\text{ReO}_3$  started at 50 °C, as evidenced by the appearance of new  $\text{Cp-H}$  signals at lower field than those of the corresponding  $\text{Cp}^*\text{Re}(\text{CO})_3$  complex with some exceptions: the formation of **1b** occurred only at 70 °C, and the 1,2,4-tri-isopropylcyclopentadienyl trioxo-rhenium complex (*vide infra*) was not detected at all. Similar experiments were also conducted with aryl-substituted 1,2,3,4-tetraphenylcyclopentadienyl tricarbonylrhenium,  $(\text{CpPh}_4\text{H})\text{Re}(\text{CO})_3$ , in benzene at 50–80 °C or with excess of  $t\text{BuOOH}$  (12 equiv), but no conversion was observed. Increasing the reaction temperature up to 100 °C in toluene- $d_8$  also did not afford the desired  $(\text{CpPh}_4\text{H})\text{ReO}_3$ , albeit a small amount of  $(\text{CpPh}_4\text{H})\text{Re}(\text{CO})_3$  was converted (ca. 20–30%, not quantified exactly).

The obtained reaction profiles of the formation of  $\text{Cp}^*\text{ReO}_3$  complexes (**1b–2b** and **4b–7b**) from the corresponding  $\text{Cp}^*\text{Re}(\text{CO})_3$  complexes are depicted in Figures 1–3. There

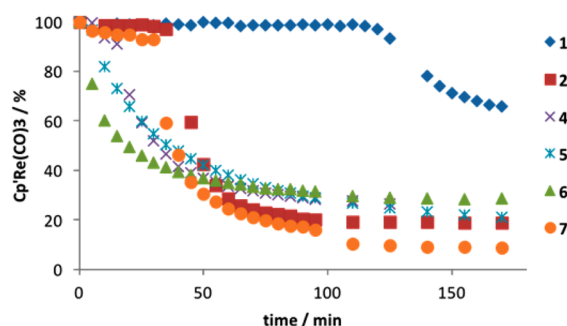


**Figure 1.** Depletion of  $\text{Cp}^*\text{Re}(\text{CO})_3$  under oxidation conditions at 50 °C in  $\text{C}_6\text{D}_6$ . The  $\text{Cp}^*\text{Re}(\text{CO})_3$  (**1a**) reaction was followed at 70 °C, and its conversion reached a constant value (ca. 57%) in 4 h.

was an induction period for all the complexes, except for the formation of **6b**. After this time, a sudden increase of the reaction rate was observed to reach nearly the optimal yield for  $\text{Cp}^*\text{ReO}_3$  in a very short time (see Figure 2). This varying induction period (10–45 min) under exactly the same reaction conditions is somewhat surprising and is probably indicative of a radical chain reaction starting from  $t\text{BuO}^\bullet$  radicals. In all cases, there is a substantial amount of unidentified missing rhenium components, suggesting parallel decomposition pathways. Many different additional  $^1\text{H}$  NMR signals ranging from 1 to

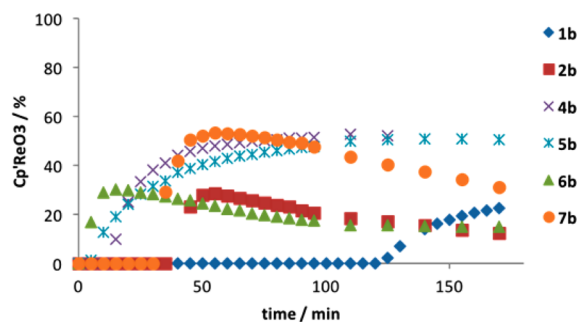


**Figure 2.** Formation of  $\text{Cp}^*\text{ReO}_3$  under oxidation conditions at 50 °C in  $\text{C}_6\text{D}_6$ .  $\text{Cp}^*\text{ReO}_3$  (**1b**) formation was followed at 70 °C, and it reached a constant value (ca. 28%) in 4 h.

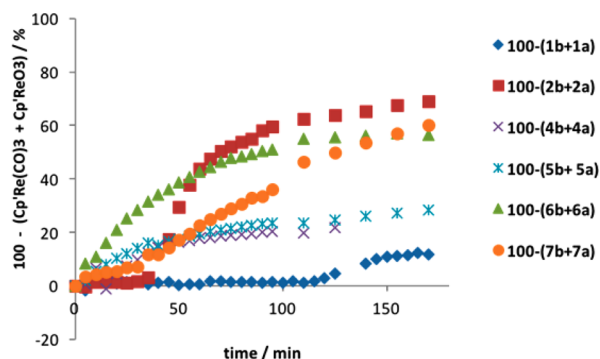


**Figure 3.** Sum of unidentified rhenium components ( $100 - (\text{Cp}^*\text{Re}(\text{CO})_3 + \text{Cp}^*\text{ReO}_3)$  %) under *in situ*  $^1\text{H}$  NMR oxidation reaction conditions at 50 °C in  $\text{C}_6\text{D}_6$ . The reaction starting from  $\text{Cp}^*\text{Re}(\text{CO})_3$  (**1a**) was followed at 70 °C.

10 ppm are found in the spectra, and these were tentatively assigned to oxidation products originating from the  $\text{Cp}^*$ -ligand.

Remarkably, the previously reported trioxo-rhenium complexes **1b**, **4b**, and **5b** were observed to be stable under these oxidation reaction conditions: their concentration reaches a plateau and does not decay under prolonged heating. Moderate product yields of 52% and 50% were obtained (by NMR experiments) for **4b** and **5b** corresponding to the conversion of **4a** and **5a** in 74% and 80%, respectively (Figures 1 and 2). The formation of **1b** was achieved in a maximum of 28% yield out of 57% conversion at 70 °C in 4 h. In these three cases, the missing rhenium components were close to only 30%.

In contrast, the yield of complexes **2b**, **6b**, and **7b** reached a maximum yield of 28, 30, and 53%, respectively, followed by a relatively slow decay under prolonged heating (Figure 2). In the meantime, the conversion of  $\text{Cp}^*\text{Re}(\text{CO})_3$  complexes reached its final value after 3 h. For these complexes, the summed missing unidentified rhenium components account for >60% (Figure 3).

The inseparable mixture of isomers of  $(\text{Cp}^*\text{Pr}_3\text{H}_2)\text{Re}(\text{CO})_3$  (**3a'**/**3a** ratio = 73:27%) was oxidized under the same reaction conditions. The reaction profile over time showed that conversion of both isomers occurred simultaneously, but only one of the corresponding trioxo-rhenium complexes (**3b**, 10%) was observed. After 85 min, only **3a'** remained in the mixture (**3a'**/**3a** = 30:0%, based on the initial amount), and a trace amount of **3b** (1.5%) was also observed (Figure 4). To confirm the origin of **3b**, an enriched sample (**3a'**/**3a** = 95:5%) was obtained by column chromatography after heating (40 min) the mixture of **3a'**/**3a** = 73:27% under the oxidation conditions.



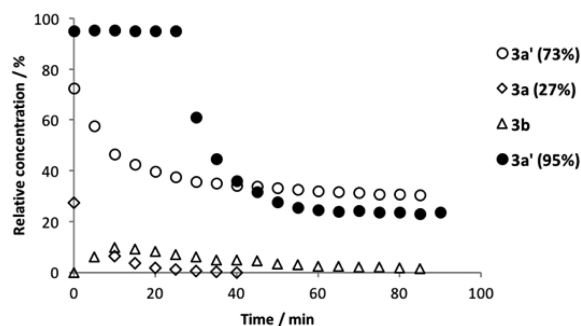


**Figure 4.** Oxidation of the isomer mixture of  $(\text{Cp}^*\text{Pr}_3\text{H}_2)\text{Re}(\text{CO})_3$  ( $3\text{a}'/3\text{a}$  ratio = 73:27%) at 50 °C in  $\text{C}_6\text{D}_6$ . The filled data point indicates the reaction corresponding to the  $3\text{a}'/3\text{a}$  ratio = 95:5%. Only the conversion of  $3\text{a}$  occurred, and no oxo-rhenium product was observed.

Subjecting the new sample ( $3\text{a}'/3\text{a}$  = 95:5%) to the same oxidation conditions showed a large consumption of  $3\text{a}'$  in 90 min ( $3\text{a}'/3\text{a}$  = 28:0%) but no appreciable formation of any trioxo-rhenium complex. This indicates that the trioxo complex  $3\text{b}$  originates from the minor isomer  $3\text{a}$ . As  $3\text{b}$  has been identified crystallographically as containing the 1,2,3-triisopropylcyclopentadienyl ligand (*vide infra*), we infer that the minor isomer  $3\text{a}$  contains the same ligand.

The oxidation reaction profiles indicate that per-alkylated ( $4\text{b}$  and  $5\text{b}$ ) or very bulky ( $1\text{b}$ )  $\text{Cp}'\text{ReO}_3$  complexes are less susceptible to decomposition under oxidative conditions, in accord with their convenient synthesis in a biphasic medium in good yields. Conversely, the less-substituted Cp-analogues ( $1\text{b}$  and  $7\text{b}$ ) were prone to decomposition and pass a maximum yield upon prolonged heating. Although the tetrahydroindenyl complex  $6\text{b}$  contains a per-alkylated Cp moiety, it still decomposed under oxidative conditions, which may be due to weaker C–H bonds in the fused cyclohexyl ring.

The reaction mechanism of the oxidative decarbonylation is not clearly understood. Kochi and co-workers proposed that an initial oxidative elimination of CO might lead to an unsaturated  $\text{Cp}^*\text{Re}(\text{CO})_2$  species, followed by quick CO exchange with oxo ligands.<sup>31,32</sup> However, Herrmann and co-workers isolated some bimetallic species containing oxo-bridges and carbonyl ligands from oxidation reactions of  $\text{Cp}^*\text{Re}(\text{CO})_3$ ,<sup>23,34</sup> which indicates a more complex reactivity behavior.

On the basis of the above *in situ* results, the alkyl-substituted  $\text{Cp}'\text{ReO}_3$   $1\text{b}$ ,  $3\text{b}$ , and  $6\text{b}$  were isolated on a preparative scale. These reactions were performed under  $\text{N}_2$  atmosphere using a

preheated oil bath at 50 °C, and the optimal reaction time as determined by NMR was applied (see [Experimental Section](#)). After the reaction, the mixture was cooled in an ice bath followed by washings with water. This allows the removal of the main decomposition product  $\text{HReO}_4$ , evidenced by an acidic ( $\text{pH} \sim 1$ ) aqueous phase, and any water-soluble oxidized organics. Furthermore, either repeated crystallization by adding hexane or pentane, or column chromatography followed by crystallization afforded pure  $\text{Cp}'\text{ReO}_3$  ( $2\text{b}$ ,  $3\text{b}$ , and  $6\text{b}$ ) as yellow crystals. The overall isolated yields are  $2\text{b}$  (18%),  $3\text{b}$  (4%), and  $6\text{b}$  (36%) (see [Experimental Section](#) for more details).

All newly synthesized  $\text{Cp}'\text{ReO}_3$  complexes ( $2\text{b}$ ,  $3\text{b}$ ,  $6\text{b}$ , and  $7\text{b}$ ) were characterized by NMR spectroscopy. All  $^1\text{H}$  NMR signals, particularly the distinct Cp–H resonances, are shifted to a low field region compared to the signals in the corresponding  $\text{Cp}'\text{Re}(\text{CO})_3$  complexes. Furthermore, ESI-MS analysis showed protonated molecular species either with or without the coordination of additives like pyridine.

The solid-state FT-IR spectra of the  $\text{Cp}'\text{ReO}_3$  complexes display the typical Re–O bands in the range of 800–950  $\text{cm}^{-1}$  and no ReC–O (1880–2010  $\text{cm}^{-1}$ ) bands. The antisymmetrical and symmetrical Re–O stretching vibrations of the  $(\text{ReO}_3)$  moiety in  $1\text{b}$ – $7\text{b}$  are typically observed in the range of 869–884 and 907–917  $\text{cm}^{-1}$ , respectively.<sup>39</sup> The  $(\text{Re–O})_{\text{asym}}$  band of the less-substituted  $2\text{b}$  (882  $\text{cm}^{-1}$ ) and  $3\text{b}$  (884  $\text{cm}^{-1}$ ) are found at slightly higher energy than that of  $1\text{b}$  (877  $\text{cm}^{-1}$ ); this band for these three complexes appear at higher energy than that for the per-alkylated complexes  $4\text{b}$ – $6\text{b}$  (869–875  $\text{cm}^{-1}$ ) ([Table 1](#)). This suggests that the  $\text{Re}=\text{O}$  multiple bond is weakened by strongly donating Cp-ligands. The complex  $7\text{b}$  lies in between these two types: an identical  $(\text{Re–O})_{\text{asym}}$  vibration at 877  $\text{cm}^{-1}$  for both  $1\text{b}$  and  $7\text{b}$  indicates that they are comparable in terms of electronics. However, the lower symmetry experienced by the bulkier  $1\text{b}$  is reflected by the higher-energy  $(\text{Re–O})_{\text{sym}}$  vibrations at 917  $\text{cm}^{-1}$  compared to that of the highly symmetrical  $7\text{b}$  ( $(\text{Re–O})_{\text{sym}}$  = 910  $\text{cm}^{-1}$ ). The spectral differences between the  $5\text{b}$ <sup>21</sup> and  $4\text{b}$ <sup>35</sup> have been interpreted in a similar way by lowering symmetry.

The X-ray crystal structures of  $2\text{b}$ ,  $3\text{b}$ ,  $6\text{b}$ , and  $7\text{b}$  all display a three-legged “piano-stool” geometry similar to that of the literature reported complexes  $1\text{b}$ ,  $4\text{b}$ , and  $5\text{b}$  ([Figure 5](#)). All of the Re–O bond distances are in the range of 1.7209(15)–1.735(4) Å for  $1\text{b}$ – $7\text{b}$ , except for the slight deviations previously reported for  $5\text{b}$  (1.664(4)–1.716(4) Å). Also, the bond angles in  $4\text{b}$  ( $\text{O–Re–O}$  = 103.7(6)–110.1(1)°) are larger

**Table 1.** Selected Analytical Data of  $\text{Cp}'\text{Re}(\text{CO})_3$  Complexes of  $1\text{a}$ – $7\text{a}$

$\text{Cp}'\text{ReO}_3$	IR ( $\text{cm}^{-1}$ ) <sup>a</sup> Re–O	X-ray crystal structure (Å/deg)			
		Cp–Re <sup>c</sup>	$\Delta^f$	Re–O	O–Re–O
$1\text{b}^b$	877, 917	2.0830(8)	0.032	1.7239(15)–1.7267(14)	103.86(8)–105.39(8)
$2\text{b}$	882, 916	2.068(3)	0.040	1.725(5)–1.735(4)	103.82(19)–105.1(3)
$3\text{b}$	884, 919	2.0637(8)	0.059	1.7209(15)–1.7281(14)	104.41(7)–105.82(9)
$4\text{b}^c$	869, 907	2.023(4) (2.032(4))	0.028 (0.046)	1.73(1)–1.744(1)	103.7(6)–110(1)
$5\text{b}^d$	875, 915	2.076(4)	0.051	1.664(4)–1.716(4)	104.7(2)–106.7(2)
$6\text{b}$	875, 909	2.062(4)	0.032	1.724(4)–1.733(2)	105.35(17)–105.89(15)
$7\text{b}$	877, 910	2.0628(15)	0.054	1.729(3)–1.733(2)	105.01(16)–105.74(11)

<sup>a</sup>IR data recorded by directly measuring the solid samples (no KBr or solvent). <sup>b</sup>Ref 17. <sup>c</sup>Ref 35. The earlier reported highly symmetrical complex  $4\text{b}$  ( $\text{Cp}^*\text{ReO}_3$ ) exhibited both crystal twinning and disorder,<sup>35</sup> precluding accurate metric determination <sup>d</sup>Ref 21. <sup>e</sup>Distance between the ring centroid and the metal. <sup>f</sup>Ring slippage  $\Delta$  is defined as the distance between the ring centroid and the perpendicular projection of the metal on the least-squares plane of the ring.

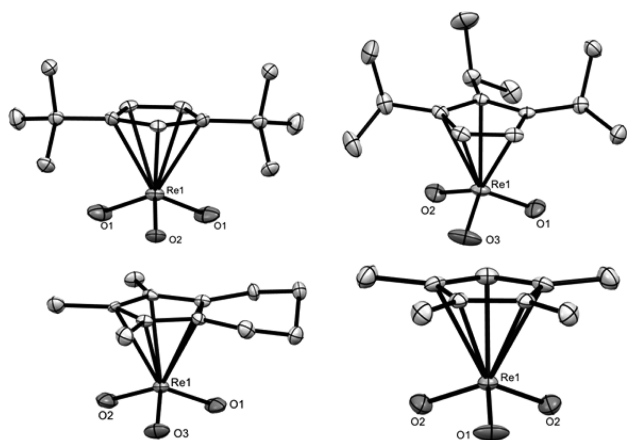


**Figure 5.** Molecular structures of **2b** (top left), **3b** (top right), **6b** (bottom left), and **7b** (bottom right) in the crystal, drawn at the 50% probability level. Hydrogen atoms are omitted for clarity. Complexes **2b** and **7b** are located on a crystallographic mirror plane.

than that in the other  $\text{Cp}^*\text{ReO}_3$  complexes ( $\text{O}-\text{Re}-\text{O} = 103.8(2)-105.0(2)^\circ$ ).

The Cp-centroid distance to rhenium (Cp–Re) in all of the  $\text{Cp}^*\text{ReO}_3$  complexes (**2b–7b**) was found in the range of 2.062(4)–2.0830(8) Å, which is significantly longer than the corresponding  $\text{Cp}^*\text{Re}(\text{CO})_3$  analogues (1.9538(6)–1.959(8) Å). This is due to the replacement of  $\pi$ -electron accepting CO ligands by  $\pi$ -electron donating oxo ligands.

In all cases, the  $\eta^5$ -Cp bonded Cp-ring is perfectly planar with a very small ring-slippage of  $\Delta = 0.032-0.059$  Å ( $\Delta$  is the distance between the ring centroid and the perpendicular projection of the metal on the least-squares plane of the ring).<sup>36</sup> This commonly occurring slight ring-slippage in  $\text{Cp}^*\text{ReO}_3$  has been attributed to the *trans*-influence of the  $\pi$ -electron donating oxo ligands.<sup>26,37</sup> The molecules of **2b** and **7b** are located on exact, crystallographic mirror planes, which pass through a C–Re–O plane. In **3b**, the Re–C(Cp<sup>i</sup>Pr) bond lengths (2.4039(17)–2.4244(17) Å) of the substituted Cp-carbons are significantly longer than those of the unsubstituted Cp-carbons (Re–C(CpH): 2.3592(17)–2.3679(18) Å). This might be due to the highly asymmetric steric bulk. In the case of **6b**, the typical puckered conformation of the fused cyclohexyl group is observed alongside torsion angles of  $-16.7(5)$  and  $-13.6(7)$  Å for the flipped methylene units (Figure 5).

In general, the spectroscopic and structural properties of the half-sandwiched “piano-stool” complexes are comparable to previously known  $\text{Cp}^*\text{ReO}_3$  complexes (**1b** and **4b–5b**). In contrast, the stability of  $\text{Cp}^*\text{ReO}_3$  complexes appears to be sensitive to the subtle changes in the Cp-substituents, which is investigated further in the next section.

**Stability of Trioxo-rhenium Species.** A striking property of the less substituted Cp trioxo-rhenium complexes (**2b**, **3b**, **6b**, and **7b**) is their relative instability in comparison to the  $\text{Cp}^*$  or  $\text{Cp}^{\text{ttt}}$  analogues under oxidation reaction conditions. To assess whether this arises from intrinsic thermal lability, the thermal stability of trioxo-rhenium compounds was examined in some detail. First, all pure  $\text{Cp}^*\text{ReO}_3$  complexes (**2b**, **3b**, **6b**, and **7b**) could be stored as yellow solids below 0 °C without decomposition for months even under air atmosphere. However, at room temperature (both under air and  $\text{N}_2$  atmosphere), these solids gradually turned first to dark-brown then to dark-green oily mixtures in 1–2 days.

The chemical nature of the decomposition products is not generally known. Some insight was gained from the decomposition of **2b**: a concentrated solution of **2b** (20 mg, 48 mM) was monitored in  $\text{CDCl}_3$  at RT under air. The color changed from yellow to dark-brown to purple-red and a precipitate appeared over the course of 1 day. The insoluble green solid was removed from the purple-red solution by filtration. After solvent evaporation *in vacuo*, a purple-red solid (**2c**) was obtained (12.2 mg), which was crystallized in  $\text{CHCl}_3$ /ether (2:1). Spectroscopic data for **2c** are consistent with the tetranuclear structure depicted in Figure 6, which is analogous to the previously reported, brown  $\text{Cp}^*\text{Re}_2\text{O}_3(\text{ReO}_4)_2$ .<sup>38</sup>

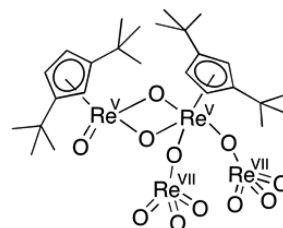


**Figure 6.** Proposed structure of **2c** formed by the decomposition of **2b**.

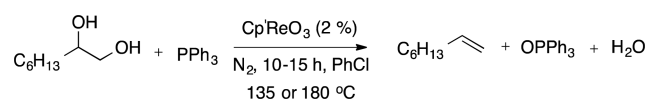
The  $^1\text{H}$  NMR spectrum of **2c** in  $\text{CDCl}_3$  displays two sets of signals belonging to two distinct  $\text{Cp}^{\text{tt}}$ -ligands in a 1:1 ratio. Further, the Re–O vibrations appear at 702, 731, 811, 874, 901, 915, and 931  $\text{cm}^{-1}$  in the IR spectrum, similar to the vibrations shown by  $\text{Cp}^*\text{Re}_2\text{O}_3(\text{ReO}_4)_2$  at 688, 700, 729, 827, 855, 899, 934, and 973  $\text{cm}^{-1}$ . An ESI-MS analysis of **2c** showed signals corresponding to a cationic species formed by loss of a neutral  $\text{ReO}_3$  fragment from **2c** ( $\text{M} - \text{ReO}_3$ )<sup>+</sup> at  $m/z = 1025.1582$  (calcd.  $m/z = 1025.1577$ ). However, the elemental analysis data of a sample of **2c** did not match with the proposed structure, which is likely due to organic impurities resulting in higher C and H percentages. The proposed structure contains two formally reduced Re(V) centers, suggesting that its formation would require a reductant; interestingly, the  $\text{Cp}^*$  analogue  $\text{Cp}^*\text{Re}_2\text{O}_3(\text{ReO}_4)_2$  was indeed formed in the presence of  $\text{PPh}_3$ . The fact that **2c** is formed from  $\text{Cp}^*\text{ReO}_3$  (**2b**) in the absence of an external reductant suggests that it may originate from a disproportionation reaction in which the  $\text{Cp}^{\text{tt}}$  ligand is oxidized and released, in agreement with the presence of “naked” trioxo-rhenium units in the structure. Moreover, tetranuclear **2c** can also be used as a catalyst in DODH reactions. At 2 mol % loading, **2c** selectively forms 1-octene (89%) out of 90% conversion of 1,2-octanediol at 180 °C for 15 h. This observation could make higher nuclear Re complexes of interest in further DODH catalyst development and in mechanistic studies.

The thermal stability of complexes **2b**, **3b**, and **6b** was also studied in solution. Solutions of each  $\text{Cp}^*\text{ReO}_3$  complex in  $\text{C}_6\text{D}_6$  (ca. 40 mM) were heated to 50 °C, and the decomposition reactions were monitored by  $^1\text{H}$  NMR. The complexes **2b** and **3b** started to decompose within 15–30 min, but per-alkylated **6b** was stable in  $\text{C}_6\text{D}_6$  even at 70 °C (30 min). Hence, complexes **2b** and **3b** are intrinsically unstable under the conditions of their preparation, which can be tentatively ascribed to the reduced steric protection of the Re center in comparison with the  $\text{Cp}^{\text{ttt}}$  (**1b**) and  $\text{Cp}^*$  (**4b**) analogues. In contrast, per-alkylated **6b** is thermally stable under the same conditions, suggesting that its decomposition arises from

reaction with the oxidant. Indeed, rapid decomposition of **6b** was observed at 50 °C in the presence of *t*BuOOH. This is likely due to the presence of weaker (secondary) C–H bonds in **6b** than in the Cp\* analogue **4b**, which would be more susceptible to H atom abstraction by radicals derived from *t*BuOOH during reaction.

**Catalytic Studies.** All Cp'ReO<sub>3</sub> complexes (**1b**–**7b**) were found to be catalytically active in the DODH of 1,2-octanediol to 1-octene. PPh<sub>3</sub> (1.1 equiv) was used as the stoichiometric reductant in chlorobenzene at 180 °C or 135 °C to completely convert 1,2-octanediol in 12–15 h (Scheme 3).<sup>17</sup> Complexes

**Scheme 3.** Cp'ReO<sub>3</sub>-Catalyzed DODH of 1,2-Octanediol to 1-Octene in Chlorobenzene



**1b**–**3b** showed high selectivity to 1-octene (94–96%) at 135 °C, whereas a small amount of the isomerization product 2-octene (5–6%, *cis*-2-octene/*trans*-2-octene ≈ 1:1) was observed at 180 °C (Table 2). Notably, the per-alkylated

**Table 2.** Cp'ReO<sub>3</sub>-Catalyzed DODH of 1,2-Octanediol in Chlorobenzene<sup>a</sup>

catalyst	yield (%) <sup>b</sup> at 180 °C				yield (%) <sup>b</sup> at 135 °C			
	1-oct	C-2-oct	T-2-oct	t (h)	1-oct	C-2-oct	T-2-oct	t (h)
<b>1b</b> <sup>c</sup>	89	3	3	12	94	1	1	15
<b>2b</b>	91	2	3	15	96	0	0	15
<b>3b</b>	95	2	2	15	94	0	0	15
<b>4b</b>	66	14	15	15	84	1	14	10
<b>5b</b>	61	9	10	12	72	2	19	15
<b>6b</b>	66	10	12	15	96	0	0	15
<b>7b</b>	70	2	4	12	96	0	0	15

<sup>a</sup>Reaction conditions: 1,2-octanediol (0.5 mmol), Cp'ReO<sub>3</sub> catalyst (0.01 mmol, 2 mol % loading), mesitylene (0.5 mmol, internal standard), PPh<sub>3</sub> (0.55 mmol), PhCl (5 mL, 100 mM based on diol), and N<sub>2</sub> atmosphere. <sup>b</sup>Determined by GC. Complete conversion to 1,2-octanediol. 1-oct/C-2-oct/T-2-oct = 1-octene/*cis*-2-octene/*trans*-2-octene. <sup>c</sup>Literature reported data in ref 20.

complexes **4b**–**6b** afforded a significant amount of 2-octene products (19–29%, *cis*-2-octene/*trans*-2-octene ≈ 1) at 180 °C and at 61–66% 1-octene formation. At 135 °C, **6b** and **7b** very selectively gave 1-octene (96%), but **4b** and **5b** produced substantial amounts of *trans*-2-octene (14–19%) together with 1-octene (72–84%).

Therefore, a high reaction temperature promotes the formation of 2-octene in all cases as reported previously for **1b**, but the reason why per-alkylated (i.e., highly electron donating) Cp-substituted catalysts (**4b**–**6b**) significantly facilitate the formation of the formal isomerization product is unclear. Control experiments carried out at 180 °C for 15 h starting from 1-octene in chlorobenzene in the presence of **4b** (2 mol %) did not show any isomerization product. However, under catalytic conditions, i.e., including 1.1 equiv of PPh<sub>3</sub>, 22% of 1-octene was isomerized to a mixture of *cis*-2-octene (12%) and *trans*-2-octene (10%) at 180 °C in 15 h. Therefore, a (reduced) rhenium species formed during the course of the DODH reaction is likely to be responsible for the resulting 2-octene products.

Reaction profiles were recorded at 135 °C for the best performing catalysts **2b** and **6b** and for the benchmark catalysts **1b** and **4b** (Figure 7). In general, an apparent zero-order

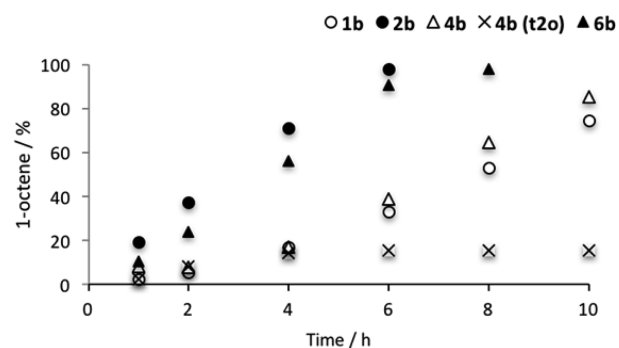


**Figure 7.** DODH reaction profile for 1,2-octanediol conversion to 1-octene at 135 °C. In the case of Cp<sup>III</sup>ReO<sub>3</sub>, 23% of 1,2-octanediol remained after 10 h. For **4b**, 15% *trans*-2-octene was formed as a side-product after 10 h, which is denoted as **4b** (**t2o**) in the figure.

reaction was observed consistent with the rate-limiting extrusion of olefin from the Re-diolate.<sup>40</sup> An induction period was observed for **1b** and **4b**, suggesting that the trioxo-rhenium complex might act as a precatalyst and not part of the real DODH cycle. Abu-Omar and co-workers recently reported on similar observations, i.e., a zero-order rate and an induction period in MTO-catalyzed DODH reactions.<sup>10</sup> It may thus be that related species are involved in these reactions.

Except for **4b** (and **5b**), which produced a significant amount of 2-octene product, the other catalysts were highly selective to yield 1-octene at 135 °C. The formation of *trans*-2-octene for **4b** mainly took place at the start of the reaction, which is coupled with an apparent induction period. This indicates an initially formed rhenium species would facilitate this reaction pathway. The amount of *trans*-2-octene remained the same after some time, while 1-octene formation gradually increased between 2–4 h (Figure 7). **1b** only gave 1-octene in 74% after 10 h with traces of 2-octene isomers out of 77% diol conversion. Interestingly, the catalysts **2b** and **6b** were found to act as much faster DODH catalysts to obtain >96% of 1-octene within 6 and 8 h, respectively. No observable 2-octene isomers were formed in these reactions (Table 2).

The rather similar reaction rates (after the induction period) could be interpreted in terms of a common catalyst being involved for the cases shown in Figure 7. The instability of the isolated high-valent Re(VII) Cp'ReO<sub>3</sub> complexes (**2b**, **3b**, **6b**, and **7b**) at high temperatures may indeed point to the formation of such a common catalyst. However, the differences in product selectivity between the different catalysts strongly suggests that the Cp-ligands are still bound in the active species, i.e., the Cp'ReO<sub>3</sub> species do not simply decompose to a common catalyst. This apparent discrepancy can be resolved by considering the fact that both the reduction of the Cp'ReO<sub>3</sub> species to Cp'ReO<sub>2</sub> and the subsequent condensation reaction with the diol substrate are rapid at room temperature already.<sup>17b</sup> Therefore, Cp'ReO<sub>3</sub> cannot be the resting state in the DODH reaction, which takes several hours at 135 °C. Under the catalytic reaction conditions with excess reductant, it therefore is most plausible that the starting Cp'ReO<sub>3</sub> species are transformed into either a mononuclear, Cp'-ligated resting state species, with the corresponding mono-oxo Re(V)diolate being a likely candidate, or into (Cp'-ligated) reduced or mixed



valent multinuclear Re-oxo or Re-diolate species. Further experimental inquiries are required to delineate these speculative DODH reaction intermediates.

## CONCLUSIONS

Multiply substituted Cp-based trioxo-rhenium complexes ( $\text{Cp}^*\text{ReO}_3$ ) were synthesized by oxidative decarbonylation of the corresponding Cp-based tricarbonyl rhenium complexes, either by using aqueous  $\text{H}_2\text{O}_2$  or  $t\text{BuOOH}$  as the oxidant. *In situ* NMR experiments for the reaction with  $t\text{BuOOH}$  were carried out at 50 °C to observe a maximum build up (up to 55%) followed by decomposition of the  $\text{Cp}^*\text{ReO}_3$  complexes at an extended reaction time. The per-alkylated  $\text{Cp}^*\text{ReO}_3$  and  $(\text{CpEtMe}_4)\text{ReO}_3$  complexes were exceptionally stable under these conditions showing no decomposition. Using the optimized oxidation reaction conditions (ca. 30 min), the synthesis of  $(\text{Cp}^t\text{Bu}_2\text{H}_3)\text{ReO}_3$  (**2b**, 18%),  $(\text{Cp}^i\text{Pr}_3\text{H}_2)\text{ReO}_3$  (**3b**, 4%),  $(1,2,3\text{-Me}_3(\text{tetrahydroindenyl}))\text{ReO}_3$  (**6b**, 36%), and  $(\text{CpMe}_4\text{H})\text{ReO}_3$  (**7b**, 33%) was achieved. Spectroscopic characterization, together with X-ray crystal structure determination, showed the typical “piano-stool” half-sandwich structure of these complexes. Preliminary studies showed that the pure  $\text{Cp}^*\text{ReO}_3$  complexes **2b**, **3b**, **6b**, and **7b** are thermally labile and are prone to decomposition to multinuclear oxo-rhenium clusters.

All complexes were found active in catalytic deoxydehydration (DODH) of 1,2-octanediol to provide very good to excellent octene yields. Surprisingly, a slight modification (**6b** and **7b**) in the electron donating property of  $\text{Cp}^*$  or the steric bulkiness (**2b** and **3b**) of  $\text{Cp}^{\text{ttt}}$  (1,2,4-tritert-butylcyclopentadienyl) ligands decreased thermal stability and resulted in improved catalytic properties in comparison with those of the previously reported  $\text{Cp}^*\text{ReO}_3$  complex, leading to catalytic properties similar to those of the  $\text{Cp}^{\text{ttt}}\text{ReO}_3$  complex. Per-alkylated Cp-ligated catalysts (**4b** and **6b**) afford significantly more 2-octene isomers than their less substituted counterparts at a higher reaction temperature. At a lower temperature, **1b–3b**, as well as **6b**, provided excellent 1-octene yields without the formation of 2-octene. Following the catalytic reactions in time has provided further insight, including the presence of induction times for some and zero-order kinetics for other catalysts. These experiments also suggest the involvement of  $\text{Cp}'$ -ligated Re-species as the resting state and active species during catalysis. Accordingly, ongoing investigations in our laboratory target the development of new Cp-based trioxo-rhenium catalysts, the application of these  $\text{Cp}'\text{ReO}_3$  catalysts for the conversion of biomass-derived polyols, as well as a detailed understanding of the mechanism by which these catalysts operate in DODH reactions.

## EXPERIMENTAL SECTION

**General Considerations.** All chemicals including rhenium complexes were degassed either by exposure *in vacuo* or freeze–pump–thaw cycles. Benzene and THF were distilled from Na/benzophenone. Toluene, THF, and acetonitrile solvents were obtained from a MBraun MB SPS-800 and stored over 4 Å molecular sieves. Unless otherwise stated, all other commercial chemicals were used without further purification. NMR spectra were recorded on a Varian VNMRS400 (400 MHz) at 298 K. Infra-red spectra were recorded using a PerkinElmer Spectrum One FT-IR spectrometer in the range of 650–4000  $\text{cm}^{-1}$ . ESI-MS spectra were recorded using a Waters LCT Premier XE instrument. GC-MS spectra were recorded on a PerkinElmer Clarus 680 Gas chromatograph, equipped with a PerkinElmer Elite SMS column (15m  $\times$  0.25 mm ID  $\times$  0.25 mm),

and a PerkinElmer Clarus SQ 8 T Mass Spectrometer. GC measurements were performed by using a PerkinElmer Autosystem XL gas chromatograph equipped with a PerkinElmer Elite-17 column (length = 30 m, internal diameter = 0.32 mm, and film thickness = 0.50 mm), and with a flame ionization detector. GC method: 40 °C, 5 min; 3 °C  $\text{min}^{-1}$  to 55 °C; 20 °C  $\text{min}^{-1}$  to 250 °C; and 250 °C, 10 min.

**Synthesis of  $\text{Cp}^t\text{ReO}_3$  **2b**.**  $\text{Cp}^t\text{Re}(\text{CO})_3$  (1.556 g, 3.476 mmol) was placed in a dried Schlenk flask and degassed *in vacuo* for 30 min. Then it was dissolved in benzene (65 mL), followed by the addition of  $t\text{BuOOH}$  (6.0 M in decane, 2.9 mL, 6 equiv) under a nitrogen atmosphere, and vigorous stirring. The reaction mixture was immersed into a preheated oil bath at 50 °C and allowed to react for 25 min, during which a color change from colorless to yellow-orange and the formation of gas (carbon monoxide) were observed. Subsequently, the reaction mixture was immediately cooled in an ice bath. A sample of the crude reaction mixture was analyzed by TLC and  $^1\text{H}$  NMR, which showed the formation of the desired product and approximately a 1:1 ratio of the carbonyl- and oxo-complexes. In open air, the reaction mixture was successively washed with water (2  $\times$  30 mL) and brine solution (1  $\times$  30 mL), dried over  $\text{MgSO}_4$ , and concentrated *in vacuo* (10 mL). Upon addition of cold hexane (40 mL) the product was precipitated and isolated by centrifugation and decantation of the hexane. To avoid a highly concentrated solution of **2b**, it was always left over with ca. 10 mL of solution to which cold hexane added to precipitate the product, and this procedure was repeated 2 more times to collect most of the product. A bright yellow crystalline solid was obtained by combination of the product fractions (262 mg, 0.637 mmol, 18%). Crystals suitable for X-ray diffraction were grown from a  $\text{CH}_2\text{Cl}_2$ /hexane 2:1 mixture at –30 °C; the unreacted  $\text{Cp}^t\text{Re}(\text{CO})_3$  (272 mg, 0.608 mmol, 18%) and the brown oily mixture (662 mg, unidentified mixtures). In addition, the water used for the workup was shown to be strongly acidic ( $\text{pH} \leq 1$ ), which indicates the presence of perhenic acid.

$^1\text{H}$  NMR (400 MHz), 25 °C,  $\text{CDCl}_3$  (7.26 ppm): 1.43 (s, 18H,  $t\text{Bu}$ ), 6.48 (t, 1H,  $\text{Cp-H}$ ,  $^4J_{\text{H,H}} = 2.4$  Hz), 6.54 (d, 2H,  $\text{Cp-H}$ ,  $^4J_{\text{H,H}} = 2.4$  Hz) ppm.  $^1\text{H}$  NMR (400 MHz), 25 °C,  $\text{C}_6\text{D}_6$  (7.16 ppm): 1.16 (s, 18H,  $t\text{Bu}$ ), 5.89 (d, 1H,  $\text{Cp-H}$ ,  $^4J_{\text{H,H}} = 2.8$  Hz), 6.18 (t, 2H,  $\text{Cp-H}$ ,  $^4J_{\text{H,H}} = 2.8$  Hz) ppm.  $^{13}\text{C}$  NMR (400 MHz), 25 °C,  $\text{CDCl}_3$  (77.16 ppm): 30.05, 33.53, 106.71, 107.72, 140.65 ppm.  $^{13}\text{C}$  NMR (400 MHz), 25 °C,  $\text{C}_6\text{D}_6$  (127.06 ppm): 29.71, 33.12, 106.76, 107.04, 139.76 ppm. FT-IR: 661, 674, 851, 882, 898, 916, 1030, 1063, 1174, 1206, 1252, 1368, 1397, 1455, 1471, 1489, 2872, 2908, 2965, 3084, 3127  $\text{cm}^{-1}$ . ESI-MS (in  $\text{CH}_2\text{Cl}_2$  with pyridine):  $m/z = 492.1554$   $\{[\text{Cp}^t\text{ReO}_3 + \text{py} + \text{H}]^+, \text{calcd. } 492.1549\}$ . Elemental analysis calcd (%) for  $\text{C}_{13}\text{H}_{21}\text{ReO}_3$  (412.10): C 37.94, H 5.14; found, C 38.42, H 5.18.

**Synthesis of  $(\text{Cp}^i\text{Pr}_3\text{H}_2)\text{ReO}_3$  **3b**.** The liquid isomer mixture of  $(\text{Cp}^i\text{Pr}_3\text{H}_2)\text{Re}(\text{CO})_3$  (1.682 g, 3.644 mmol) was introduced into a dried Schlenk flask and degassed *in vacuo* for 30 min. Then, it was dissolved in benzene (80 mL), followed by the addition of 6 equiv of  $t\text{BuOOH}$  (6.0 M in decane, 3.8 mL, 22.8 mmol, 6.2 equiv) under a nitrogen atmosphere and vigorous stirring. The reaction mixture was immersed into a preheated oil bath at 50 °C and allowed to react for 15 min, during which a color change from very light brown to bright yellow was observed. Subsequently, the reaction mixture was immediately cooled down in an ice bath. A sample of the crude reaction mixture was used for TLC, which showed the formation of a newly formed species, and the expected incomplete conversion of  $(\text{Cp}^i\text{Pr}_3\text{H}_2)\text{Re}(\text{CO})_3$ . In open air, the reaction mixture was washed with water (2  $\times$  80 mL) and brine (1  $\times$  80 mL). The separated organic layer was then dried over  $\text{MgSO}_4$  and concentrated *in vacuo*. From the resulting liquid mixture (0.7241 g), the desired product was isolated over a silica column. The unreacted tricarbonyl rhenium complexes and organic side products were eluted first with petroleum ether as eluent. After that, the yellow product fraction was eluted with dichloromethane and petroleum ether (1:1). A yellow viscous liquid was obtained (0.5618 g), which contained only one trioxo-rhenium complex mixed with the high boiling organics. The product could not be precipitated at room temperature, but yellow, needle-shaped

crystals were grown (65.3 mg, 4.2%) by adding hexane (5 mL) and storing the resulting solution at  $-30\text{ }^{\circ}\text{C}$  for 3 days. The obtained crystals were suitable for X-ray crystal structure determination. Furthermore, 10% of the unreacted  $(\text{Cp}^*\text{Pr}_3\text{H}_2)\text{Re}(\text{CO})_3$  was collected from the column separation (159.4 mg, 0.345 mmol). In addition, the water used for the workup was strongly acidic ( $\text{pH} \leq 1$ ), which indicates the presence of formed perhenic acid.

$^1\text{H}$  NMR (400 MHz),  $25\text{ }^{\circ}\text{C}$ ,  $\text{CDCl}_3$  (7.26 ppm):  $\delta = 1.29$  (s, 6H, Me,  $J =$ ), 1.40 (s, 6H, Me), 1.46 (s, 6H, Me), 3.06 (two overlapping septets, 3H,  $\text{CHMe}_2$ ), 6.39 (s, 2H, Cp–H) ppm.  $^1\text{H}$  NMR (400 MHz),  $25\text{ }^{\circ}\text{C}$ ,  $\text{C}_6\text{D}_6$  (7.16 ppm): 0.81, (s, 6H, Me), 1.19 (s, 6H, Me), 1.21 (s, 6H, Me), 2.73 (sept, 1H,  $\text{CHMe}_2$ ), 2.79 (sept, 2H,  $\text{CHMe}_2$ ), 5.83 (s, 2H, Cp–H) ppm.  $^{13}\text{C}$  NMR (400 MHz),  $25\text{ }^{\circ}\text{C}$ ,  $\text{CDCl}_3$  (77.16 ppm): 20.82, 22.62, 24.35, 26.73, 26.83, 103.15, 123.37, 141.15. FT-IR: 478, 548, 607, 684, 714, 841, 861, 884, 919, 1017, 1056, 1099, 1206, 1284, 1306, 1368, 1384, 1457, 2969, 3114. ESI-MS (in  $\text{CH}_3\text{CN}$  with pyridine and  $\text{HCOOH}$  as additives):  $m/z = 506.1701$   $\{[\text{M} + \text{py} + \text{H}]^+, \text{calcd. } 506.1706\}$ . Elemental analysis calcd (%) for  $\text{C}_{14}\text{H}_{23}\text{ReO}_3$  (426.12): C 39.52, H 5.45; found, C 39.34, H 5.33.

**Synthesis of  $(1,2,3\text{-Me}_3(\text{tetrahydroindenyl}))\text{ReO}_3$  6b.**  $(1,2,3\text{-Me}_3(\text{tetrahydroindenyl}))\text{Re}(\text{CO})_3$  6a (125.0 mg, 0.304 mmol) was placed in a dried Schlenk flask and degassed *in vacuo* for 30 min. Then, it was dissolved in benzene (6.25 mL), followed by the addition of *t*BuOOH (6.0 M in decane, 0.3 mL, 6 equiv. based on rhenium) under a nitrogen atmosphere and vigorous stirring. The reaction mixture was immersed into a preheated oil bath at  $50\text{ }^{\circ}\text{C}$  and allowed to react for 20 min, during which a color change from colorless to bright yellow was observed. Subsequently, the reaction mixture was immediately cooled in an ice bath. A small sample of the crude reaction mixture was analyzed by TLC, which showed the formation of a newly formed species, and the expected incomplete conversion of 6a. In open air, the reaction mixture was washed with demineralized water ( $2 \times 7\text{ mL}$ ) and brine solution ( $1 \times 7\text{ mL}$ ). The isolated organic layer was then dried over  $\text{MgSO}_4$  and concentrated *in vacuo*. A first product fraction was isolated by precipitating  $(1,2,3\text{-Me}_3(\text{tetrahydroindenyl}))\text{ReO}_3$  in hexane at  $-30\text{ }^{\circ}\text{C}$  (yield = 21.1 mg), followed by centrifugation, and decantation. The remaining liquid, which still contained more product, was separated over a silica column. The unreacted tricarbonyl rhenium complexes and organic side products were eluted first with petroleum ether as eluent. After that, the yellow product fraction was eluted with dichloromethane and petroleum ether (1:1) as eluent (yield = 23.4 mg). Combination of the two product fractions yielded a total of yield 36% (44.5 mg, 0.113 mmol). Crystals suitable for X-ray diffraction were grown from a  $\text{CH}_2\text{Cl}_2$ /hexane (2:1) mixture at  $-30\text{ }^{\circ}\text{C}$ . The mass balance of the reaction was verified by collecting the unreacted 6a (70.8 mg, 0.172 mmol, 57%). In addition, the water used for the workup was shown to be strongly acidic ( $\text{pH} \leq 1$ ), which indicates the presence of formed perhenic acid.

$^1\text{H}$  NMR (400 MHz),  $25\text{ }^{\circ}\text{C}$ ,  $\text{CDCl}_3$  (7.26 ppm): 1.75 (m, br, 2H,  $\text{CH}_2\text{exo}$ ), 1.83 (m, br, 2H,  $\text{CH}_2\text{endo}$ ), 2.10 (s, 6H, Me), 2.21 (s, 3H, Me), 2.61 (m, br, 2H, Cp– $\text{CH}_2\text{exo}$ ), 2.73 (m, br, 2H, Cp– $\text{CH}_2\text{endo}$ ) ppm.  $^1\text{H}$  NMR (400 MHz),  $25\text{ }^{\circ}\text{C}$ ,  $\text{C}_6\text{D}_6$  (7.16 ppm): 1.22 (m, br, 2H,  $\text{CH}_2\text{exo}$ ), 1.56 (m, br, 2H,  $\text{CH}_2\text{endo}$ ), 1.57 (s, 6H, Me), 1.71 (s, 3H, Me), 1.90 (m, br, 2H, Cp– $\text{CH}_2\text{exo}$ ), 2.46 (m, br, 2H, Cp– $\text{CH}_2\text{endo}$ ) ppm.  $^{13}\text{C}$  NMR (400 MHz),  $25\text{ }^{\circ}\text{C}$ ,  $\text{C}_6\text{D}_6$  (117.06 ppm): 9.60, 9.63, 21.51, 21.55, 110.40, 116.37, 121.38, 122.08 ppm. IR: 790, 813, 875, 909, 1028, 1143, 1192, 1242, 1332, 1366, 1378, 1422, 1714, 2865, 2936,  $3401\text{ cm}^{-1}$ . ESI-MS (in  $\text{CH}_3\text{CN}$  with pyridine):  $m/z = 460.0936$   $\{[\text{M} + \text{Na} + \text{CH}_3\text{CN}]^+, \text{calcd. } 460.0899\}$ ;  $^{51}\text{V}$  476.1229  $\{[\text{M} + \text{pyridine} + \text{H}]^+, \text{calcd. } 476.1236\}$ .

**Synthesis of  $(\text{Me}_4\text{CpH})\text{ReO}_3$  7b.**  $(\text{Me}_4\text{CpH})\text{Re}(\text{CO})_3$  7a (0.7 g, 1.8 mmol) was degassed in a dried Schlenk flask by stirring for 30 min *in vacuo*, followed by the addition of benzene (35 mL) and  $\text{H}_2\text{O}_2$  (35% in water, 3.5 mL, 20 equiv). The resulting mixture was refluxed ( $75\text{ }^{\circ}\text{C}$ ) for 1 h, after which the yellow organic layer was separated from the water layer, which was extracted with benzene ( $2 \times 5\text{ mL}$ ) in open air. Then, the organic layer was washed with water ( $2 \times 50\text{ mL}$ ), 5%  $\text{NaHCO}_3$  solution ( $1 \times 50\text{ mL}$ ), and brine ( $2 \times 50\text{ mL}$ ), before it was dried over  $\text{MgSO}_4$ . After the removal of benzene *in vacuo*, 7b was obtained as a yellow solid in 33% yield (0.209 g), and traces of oily

impurities were seen at the sides of the flask. An analytically pure sample was obtained by recrystallization in a 2:1 mixture of dichloromethane/hexane (1/0.5 mL) at  $-30\text{ }^{\circ}\text{C}$ .  $^1\text{H}$  NMR (400 MHz),  $\text{CDCl}_3$  (7.26 ppm): 2.08 (s, 6H, Me), 2.32 (s, 6H, Me), 5.95 (s, 1H, CpH).  $^{13}\text{C}$  NMR (400 MHz),  $\text{CDCl}_3$  (77.16 ppm): 10.52, 12.05, 104.64, 122.52, 124.88 ppm. ESI-MS (in  $\text{CH}_3\text{CN}$ ): calcd. for  $[\text{C}_9\text{H}_{13}\text{ReO}_3 + \text{H}]^+$ : 357.0501; found: 357.0434. Elemental analysis calcd. (%) for  $\text{C}_9\text{H}_{13}\text{ReO}_3$  (355.45): C 30.42, H 3.69; found, C 29.86, H 3.93.

**General Procedure for Tricarbonyl Rhenium Oxidation Profile Determination.** Unless otherwise described, all reaction mixtures were prepared in a Teflon-capped Young-type NMR tube, which was placed in a Schlenk flask under a nitrogen atmosphere. The actual reactions were performed inside a Varian 400 MHz spectrometer with variable-temperature programming. The intended  $\text{Cp}^*\text{Re}(\text{CO})_3$  (10 mg) and 1,4-di-*tert*-butylbenzene internal standard (1 equiv) were degassed *in vacuo* for 30 min, and then dissolved in degassed  $\text{C}_6\text{D}_6$  (0.5 mL). *t*BuOOH (6.0 M in decane, 6 equiv) was added by using a calibrated microliter syringe. Immediately, the NMR tube was closed inside the Schlenk flask under a counterflow of nitrogen, and the resulting mixture was shaken thoroughly. The initial quantities of the reaction mixture were determined by recording a  $^1\text{H}$  NMR spectrum at  $25\text{ }^{\circ}\text{C}$ . For a second initial quantity check, whenever necessary, the temperature was increased to  $40\text{ }^{\circ}\text{C}$  for approximately 15 min, in order to shift the broad peroxide peak sufficiently below 7 ppm, so that overlap with the peak of 1,4-di-*tert*-butylbenzene was avoided. After that, the temperature was increased to  $50\text{ }^{\circ}\text{C}$ , except for  $\text{Cp}^*\text{Re}(\text{CO})_3$  that required  $70\text{ }^{\circ}\text{C}$  for the reaction to occur. A preacquisition delay  $^1\text{H}$  NMR recording with intervals of 5 min was programmed to follow the change in quantities of starting material and products during the reaction. Immediately after the reaction, a sample of the crude reaction mixture was dissolved in hexane and analyzed by GC-MS. The concentrations were calculated based on the integrals of Cp–H signals and in some cases methyl signals in the  $^1\text{H}$  NMR spectra.

**Procedure for the Decomposition Study of 2b to 2c.** In a Schlenk flask,  $\text{Cp}^*\text{ReO}_3$  (20 mg, 0.0486 mmol) was dissolved in  $\text{CDCl}_3$  (1.0 mL) under a nitrogen atmosphere and left at room temperature. Within 1 day, the mixture had turned completely dark, bearing a red-brown solution and the insoluble dark green solid. Intermediate  $^1\text{H}$  NMR analyses showed the formation of many decomposition products in the solid, and a new complex species in the liquid. The red-brown solution was filtered, and evaporated *in vacuo* to yield a dark red solid (12.2 mg). This solid was then recrystallized from a mixture of chloroform and diethyl ether (2:1) at  $-30\text{ }^{\circ}\text{C}$ , and dark red block-shaped crystals of 2c were obtained.

$^1\text{H}$  NMR (400 MHz),  $25\text{ }^{\circ}\text{C}$ ,  $\text{CDCl}_3$  (7.26 ppm): 1.19 (s, 18H, *t*Bu,  $^4J_{\text{H,H}} = 2.4\text{ Hz}$ ), 1.49 (s, 18H, *t*Bu), 5.67 (t, 1H, Cp–H,  $^4J_{\text{H,H}} = 2.4\text{ Hz}$ ), 6.05 (d, 2H, Cp–H,  $^4J_{\text{H,H}} = 2.4\text{ Hz}$ ), 6.13 (d, 2H, Cp–H,  $^4J_{\text{H,H}} = 2.4\text{ Hz}$ ), 6.52 (t, 1H, Cp–H,  $^4J_{\text{H,H}} = 2.4\text{ Hz}$ ) ppm.  $^{13}\text{C}$  NMR (400 MHz),  $25\text{ }^{\circ}\text{C}$ ,  $\text{CDCl}_3$  (77.16 ppm): 30.30, 30.78, 33.95, 34.79, 77.37, 96.46, 96.92, 107.87, 108.25, 134.18, 137.13 ppm. FT-IR: 702, 731, 811, 874, 901, 915, 931, 1070, 1167, 1251, 1363, 1464, 1702, 2961,  $3096\text{ cm}^{-1}$ . ESI-MS (in  $\text{CH}_2\text{Cl}_2$ ):  $m/z = 1025.1582$   $\{[(\text{Cp}^*\text{ReO})_2\text{O}(\text{ReO}_4)]^+, \text{calcd. } 1025.1577\}$ ; 1421.2621  $\{[(\text{Cp}^*\text{ReO}_2)_3\text{ReO}_3]^+, \text{calcd. } 1421.26\}$  Elemental analysis calcd (%) for  $\text{C}_{26}\text{H}_{42}\text{Re}_4\text{O}_{11}$  (1278.10): C 24.48, H 3.32; found, C 27.11, H 3.76.

**General Procedure for Catalytic Deoxydehydration.** Unless otherwise described, all reaction mixtures were prepared inside the glovebox under nitrogen atmosphere. 1,2-Octanediol (286 mg, 1.96 mmol),  $\text{PPh}_3$  (580 mg, 2.21 mmol), and mesitylene (Internal standard, 225 mg, 1.87 mmol) were dissolved in chlorobenzene (20 mL). Aliquots (5 mL) of this stock solution were added to each  $\text{Cp}^*\text{ReO}_3$  catalyst (0.01 mmol) in a 15 mL thick-walled glass pressure tube (Ace) fitted with a Teflon screw-cap. Then, the closed reaction flask was immersed into a preheated oil bath at  $135\text{ }^{\circ}\text{C}$ . At regular intervals, to plot the reaction profile, the reaction tube was cooled down in an ice bath and then warmed to room RT before taking aliquots of the reaction mixture inside the glovebox. However, the reaction was stopped only once after 15 h when the final catalytic data were needed.



The samples were diluted (ca. 10 times) with acetone (for olefins) or ethyl acetate (for diols) in open air for GC analysis. All olefinic products were known compounds and were calibrated against mesitylene for quantification. Alternatively, all the reagents (0.5 mmol substrate, 0.01 mmol catalyst, 0.55 mmol PPh<sub>3</sub>, and 0.5 mmol mesitylene) were weighed in a scintillation glass vial for the experiments carried out at 135 or 180 °C for 15 h, which also applies to the control experiments starting from 1-octene. Then, 5 mL of PhCl was used to dissolve before transferring into the pressure tubes.

**X-ray Crystal Structure Determinations.** **Compound 2b.** C<sub>13</sub>H<sub>21</sub>O<sub>3</sub>Re, *F*<sub>w</sub> = 411.50, yellow plate, 0.45 × 0.28 × 0.07 mm<sup>3</sup>, monoclinic, *P*<sub>2</sub><sub>1</sub>/*m* (no. 11), *a* = 6.3051(3), *b* = 19.3260(14), *c* = 6.3244(5) Å, β = 118.867(3)°, *V* = 674.88(8) Å<sup>3</sup>, *Z* = 2, *D*<sub>x</sub> = 2.025 g/cm<sup>3</sup>, and μ = 9.00 mm<sup>-1</sup>. 10858 Reflections were measured on a Bruker Kappa ApexII diffractometer with sealed tube and Triumph monochromator (λ = 0.71073 Å) at a temperature of 150(2) K up to a resolution of (sin θ/λ)<sub>max</sub> = 0.66 Å<sup>-1</sup>. The crystal appeared to be nonmerohedrally twinned with a 2-fold rotation about *hkl* = (0,0,1) as twin operation. Consequently, two orientation matrices were used for the integration of the intensity data with the Eval15 software.<sup>41</sup> An analytical absorption correction was performed with PLATON<sup>36</sup> (correction range 0.08–0.69) resulting in a HKLF5 file.<sup>42</sup> 1992 reflections were unique (*R*<sub>int</sub> = 0.054), of which 1983 were observed [*I* > 2σ(*I*)]. The structure was solved with automated Patterson methods using the program DIRDIF-08.<sup>43</sup> Least-squares refinement was performed with SHELXL-2013<sup>44</sup> against the *F*<sup>2</sup> of all reflections. Non-hydrogen atoms were refined freely with anisotropic displacement parameters. All hydrogen atoms were included in calculated positions and refined with a riding model. 86 parameters were refined with no restraints. *R*<sub>1</sub>/*wR*<sub>2</sub> [*I* > 2σ(*I*)]: 0.0260/0.0648. *R*<sub>1</sub>/*wR*<sub>2</sub> [all refl.]: 0.0261/0.0649. *S* = 1.179. Batch scale factor for the second twin component BASF = 0.2995(16). Residual electron density between −1.49 and 2.73 e/Å<sup>3</sup>. Geometry calculations and checking for higher symmetry were performed with the PLATON program.<sup>36</sup>

**Compound 3b.** C<sub>14</sub>H<sub>23</sub>O<sub>3</sub>Re, *F*<sub>w</sub> = 425.52, yellow block, 0.26 × 0.11 × 0.08 mm<sup>3</sup>, monoclinic, *P*<sub>2</sub><sub>1</sub>/*n* (no. 14), *a* = 8.5282(2), *b* = 12.0181(3), *c* = 14.2586(3) Å, β = 93.993(1)°, *V* = 1457.85(6) Å<sup>3</sup>, *Z* = 4, *D*<sub>x</sub> = 1.939 g/cm<sup>3</sup>, and μ = 8.33 mm<sup>-1</sup>. 35418 Reflections were measured on a Bruker Kappa ApexII diffractometer with sealed tube and Triumph monochromator (λ = 0.71073 Å) at a temperature of 150(2) K up to a resolution of (sin θ/λ)<sub>max</sub> = 0.65 Å<sup>-1</sup>. Intensity data were integrated with the Eval15 software.<sup>41</sup> Analytical absorption correction and scaling was performed with SADABS<sup>45</sup> (correction range 0.35–0.64). 3343 Reflections were unique (*R*<sub>int</sub> = 0.015), of which 3257 were observed [*I* > 2σ(*I*)]. The structure was solved with SHELXT.<sup>46</sup> Least-squares refinement was performed with SHELXL-2014<sup>44</sup> against the *F*<sup>2</sup> of all reflections. Non-hydrogen atoms were refined freely with anisotropic displacement parameters. All hydrogen atoms were located in difference Fourier maps. Hydrogen atoms H4 and H5 of the Cp ring were refined freely with isotropic displacement parameters. All other hydrogens were refined with a riding model. 178 parameters were refined with no restraints. *R*<sub>1</sub>/*wR*<sub>2</sub> [*I* > 2σ(*I*)]: 0.0110/0.0263. *R*<sub>1</sub>/*wR*<sub>2</sub> [all refl.]: 0.0115/0.0264. *S* = 1.090. Extinction parameter EXTI = 0.00048(4). Residual electron density between −0.90 and 1.39 e/Å<sup>3</sup>. Geometry calculations and checking for higher symmetry were performed with the PLATON program.<sup>36</sup>

**Compound 6b.** C<sub>12</sub>H<sub>17</sub>O<sub>3</sub>Re, *F*<sub>w</sub> = 395.45, yellow-green block, 0.23 × 0.13 × 0.11 mm<sup>3</sup>, orthorhombic, *Pna*2<sub>1</sub> (no. 33), *a* = 10.9327(4), *b* = 8.1327(2), *c* = 13.2961(4) Å, *V* = 1182.18(6) Å<sup>3</sup>, *Z* = 4, *D*<sub>x</sub> = 2.222 g/cm<sup>3</sup>, and μ = 10.27 mm<sup>-1</sup>. 13606 reflections were measured on a Bruker Kappa ApexII diffractometer with sealed tube and Triumph monochromator (λ = 0.71073 Å) at a temperature of 150(2) K up to a resolution of (sin θ/λ)<sub>max</sub> = 0.65 Å<sup>-1</sup>. The crystal was cracked into several crystal fragments. Only the intensity data of the major fragment were integrated with the Eval15 software.<sup>41</sup> Analytical absorption correction and scaling were performed with SADABS<sup>45</sup> (correction range 0.21–0.57). 2709 reflections were unique (*R*<sub>int</sub> = 0.016), of which 2544 were observed [*I* > 2σ(*I*)]. The structure was solved with direct methods using SIR-97.<sup>47</sup> Least-squares refinement was performed with SHELXL-2014<sup>44</sup> against the *F*<sup>2</sup> of all reflections.

Non-hydrogen atoms were refined freely with anisotropic displacement parameters. All hydrogen atoms were located in difference Fourier maps and refined with a riding model. 178 parameters were refined with 1 restraint (floating origin). *R*<sub>1</sub>/*wR*<sub>2</sub> [*I* > 2σ(*I*)]: 0.0098/0.0227. *R*<sub>1</sub>/*wR*<sub>2</sub> [all refl.]: 0.0112/0.0230. *S* = 1.065. Flack parameter<sup>48</sup> *x* = 0.291(11). Residual electron density was between −0.49 and 0.25 e/Å<sup>3</sup>. Geometry calculations and checking for higher symmetry were performed with the PLATON program.<sup>36</sup>

**Compound 7b.** C<sub>9</sub>H<sub>13</sub>O<sub>3</sub>Re, *F*<sub>w</sub> = 355.39, yellow plate, 0.08 × 0.05 × 0.03 mm<sup>3</sup>, orthorhombic, *Pnma* (no. 62), *a* = 5.9964(3), *b* = 13.1856(7), *c* = 12.0268(7) Å, *V* = 950.91(9) Å<sup>3</sup>, *Z* = 4, *D*<sub>x</sub> = 2.482 g/cm<sup>3</sup>, and μ = 12.75 mm<sup>-1</sup>. 13014 reflections were measured on a Bruker Kappa ApexII diffractometer with sealed tube and Triumph monochromator (λ = 0.71073 Å) at a temperature of 150(2) K up to a resolution of (sin θ/λ)<sub>max</sub> = 0.70 Å<sup>-1</sup>. Intensity data were integrated with the Saint software.<sup>49</sup> Multiscan absorption correction and scaling were performed with SADABS<sup>45</sup> (correction range 0.32–0.43). 1452 reflections were unique (*R*<sub>int</sub> = 0.033), of which 1280 were observed [*I* > 2σ(*I*)]. The structure was solved with direct methods using SHELXS-97.<sup>50</sup> Least-squares refinement was performed with SHELXL-97<sup>50</sup> against the *F*<sup>2</sup> of all reflections. Non-hydrogen atoms were refined freely with anisotropic displacement parameters. All hydrogen atoms were located in difference Fourier maps. Hydrogen atom H1 of the Cp ring was refined freely with an isotropic displacement parameter. All other hydrogens were refined with a riding model. 69 parameters were refined with no restraints. *R*<sub>1</sub>/*wR*<sub>2</sub> [*I* > 2σ(*I*)]: 0.0189/0.0416. *R*<sub>1</sub>/*wR*<sub>2</sub> [all refl.]: 0.0251/0.0434. *S* = 1.067. Residual electron density was between −1.07 and 2.13 e/Å<sup>3</sup>. Geometry calculations and checking for higher symmetry were performed with the PLATON program.<sup>36</sup>

## ■ ASSOCIATED CONTENT

### ■ Supporting Information

The Supporting Information is available free of charge on the ACS Publications website at DOI: 10.1021/acs.organo-  
met.6b00120.

The NMR spectra of all the new complexes (PDF)  
X-ray data (CIF)

## ■ AUTHOR INFORMATION

### Corresponding Author

\*E-mail: R.J.M.KleinGebink@uu.nl.

### Notes

The authors declare no competing financial interest.

## ■ ACKNOWLEDGMENTS

This research has been performed within the framework of the CatchBio program. We gratefully acknowledge the support of the Smart Mix Program of The Netherlands Ministry of Economic Affairs and The Netherlands Ministry of Education, Culture, and Science. The X-ray diffractometer has been financed by The Netherlands Organization for Scientific Research (NWO). M.E.M. acknowledges funding from the European Union Seventh Framework Programme (FP7/2007–2013) under grant agreement PIFI-GA-2012-327306 (IIF-Marie Curie grant) and the Sectorplan Natuur-en Scheikunde (Tenure-track grant at Utrecht University).

## ■ REFERENCES

- (1) Adduci, L. L.; McLaughlin, M. P.; Bender, T. A.; Becker, J. J.; Gagne, M. R. *Angew. Chem., Int. Ed.* **2014**, *53*, 1646–1649.
- (2) ten Dam, J.; Hanefeld, U. *ChemSusChem* **2011**, *4*, 1017–1034.
- (3) Schlaf, M. *Dalton Trans.* **2006**, 4645–4653.
- (4) Werpy, T.; Petersen, G.; Aden, A.; Bozell, J.; Holladay, J.; White, J.; Manheim, A.; Eliot, D.; Lasure, L.; Jones, S. *Top Value Added*

*Chemicals from Biomass: Volume 1 - Results of Screening for Potential Candidates from Sugars and Synthesis Gas*, 2004.

- (5) Raju, S.; Moret, M.-E.; Klein Gebbink, R. J. M. *ACS Catal.* **2015**, *5*, 281–300.
- (6) Dethlefsen, J. R.; Fristrup, P. *ChemSusChem* **2015**, *8*, 767–775.
- (7) Boucher-Jacobs, C.; Nicholas, K. M. *Top. Curr. Chem.* **2014**, *353*, 163–184.
- (8) Shiramizu, M.; Toste, F. D. *Angew. Chem., Int. Ed.* **2012**, *51*, 8082–8086.
- (9) Shiramizu, M.; Toste, F. D. *Angew. Chem., Int. Ed.* **2013**, *52*, 12905–12909.
- (10) Liu, S.; Senocak, A.; Smeltz, J. L.; Yang, L.; Wegenhart, B.; Yi, J.; Kenttamaa, H. I.; Ison, E. A.; Abu-Omar, M. M. *Organometallics* **2013**, *32*, 3210–3219.
- (11) Yi, J.; Liu, S.; Abu-Omar, M. M. *ChemSusChem* **2012**, *5*, 1401–1404.
- (12) Herrmann, W. A.; Romão, C. C.; Fischer, R. W.; Kiprof, P.; de Méric de Bellefon, C. *Angew. Chem., Int. Ed. Engl.* **1991**, *30*, 185–186.
- (13) Herrmann, W. A.; Kühn, F. E. *Acc. Chem. Res.* **1997**, *30*, 169–180.
- (14) Herrmann, W. A.; Kühn, F. E.; Romão, C. C.; Huy, H. T.; Wang, M.; Fischer, R. W.; Kiprof, P.; Scherer, W. *Chem. Ber.* **1993**, *126*, 45–50.
- (15) Cook, G. K.; Andrews, M. A. *J. Am. Chem. Soc.* **1996**, *118*, 9448–9449.
- (16) Gable, K. P.; Zhuravlev, F. A.; Yokochi, A. F. T. *Chem. Commun.* **1998**, 799–800.
- (17) (a) Raju, S.; Jastrzebski, J. T. B. H.; Lutz, M.; Klein Gebbink, R. J. M. *ChemSusChem* **2013**, *6*, 1673–1680. (b) Raju, S.; Jastrzebski, J. T. B. H.; Lutz, M.; Witteman, L.; Dethlefsen, J. L.; Fristrup, P.; Moret, M.-E.; Klein Gebbink, R. J. M. *Inorg. Chem.* **2015**, *54*, 11031–11036. (c) Raju, S.; van Slagmaat, C. A. M. R.; Lutz, M.; Kleijn, H.; Jastrzebski, J. T. B. H.; Moret, M.-E.; Klein Gebbink, R. J. M. Manuscript in preparation.
- (18) Kühn, F. E.; Herrmann, W. A.; Hahn, R.; Elison, M.; Blümel, J.; Herdtweck, E. *Organometallics* **1994**, *13*, 1601–1606.
- (19) Herrmann, W. A.; Taillefer, M.; de Méric de Bellefon, C.; Behm, J. *Inorg. Chem.* **1991**, *30*, 3247–3248.
- (20) Högerl, M.; Kühn, F. E. *Z. Anorg. Allg. Chem.* **2008**, *634*, 1444–1447.
- (21) Okuda, J.; Herdtweck, E.; Herrmann, W. A. *Inorg. Chem.* **1988**, *27*, 1254–1257.
- (22) Kühn, F. E.; Herrmann, W. A.; Hahn, R.; Elison, M.; Blümel, J.; Herdtweck, E. *Organometallics* **1994**, *13*, 1601–1606.
- (23) Herrmann, W. A.; Voss, E.; Flöel, M. *J. Organomet. Chem.* **1985**, *297*, C5–C7.
- (24) Herrmann, W. A.; Correia, J. D. G.; Kühn, F. E.; Artus, G. R. J.; Romão, C. C. *Chem.–Eur. J.* **1996**, *2*, 168–173.
- (25) Thiel, W. R.; Fischer, R. W.; Herrmann, W. A. *J. Organomet. Chem.* **1993**, *459*, C9–C11.
- (26) Herrmann, W. A.; Okuda, J. *J. Mol. Catal.* **1987**, *41*, 109–122.
- (27) Herrmann, W. A.; Serrano, R.; Küsthardt, U.; Ziegler, M. L.; Guggolz, E.; Zahn, T. *Angew. Chem., Int. Ed. Engl.* **1984**, *23*, 515–517.
- (28) Klahn-Oliva, A. H.; Sutton, D. *Organometallics* **1984**, *3*, 1313–1314.
- (29) Gable, K. P.; Phan, T. N. *J. Organomet. Chem.* **1994**, *466*, C5–C6.
- (30) Herrmann, W. A.; Kiprof, P.; Rypdal, K.; Tremmel, J.; Blom, R.; Alberto, R.; Behm, J.; Albach, R. W.; Bock, H. *J. Am. Chem. Soc.* **1991**, *113*, 6527–6537.
- (31) Wallis, J. M.; Kochi, J. K. *Inorg. Chim. Acta* **1989**, *160*, 217–221.
- (32) Wolowiec, S.; Kochi, J. K. *Inorg. Chem.* **1991**, *30*, 1215–1221.
- (33) Szyperski, T.; Schwerdtfeger, P. *Angew. Chem., Int. Ed. Engl.* **1989**, *28*, 1228–1231.
- (34) Herrmann, W. A.; Serrano, R.; Schäfer, A.; Küsthardt, U.; Ziegler, M. L.; Guggolz, E. *J. Organomet. Chem.* **1984**, *272*, 55–71.
- (35) Burrell, A. K.; Cotton, F. A.; Daniels, L. M.; Petricek, V. *Inorg. Chem.* **1995**, *34*, 4253–4255.
- (36) Spek, A. L. *Acta Crystallogr., Sect. D: Biol. Crystallogr.* **2009**, *65*, 148–155.
- (37) Herrmann, W. A.; Herdtweck, E.; Flöel, M.; Kulpe, J.; Küsthardt, U.; Okuda, J. *Polyhedron* **1987**, *6*, 1165–1182.
- (38) Herrmann, W. A.; Serrano, R.; Küsthardt, U.; Guggolz, E.; Nuber, B.; Ziegler, M. L. *J. Organomet. Chem.* **1985**, *287*, 329–344.
- (39) Bencze, E.; Mink, J.; Németh, C.; Herrmann, W. A.; Lokshin, B. V.; Kühn, F. E. *J. Organomet. Chem.* **2002**, *642*, 246–258.
- (40) Gable, K. P.; Phan, T. N. *J. Am. Chem. Soc.* **1994**, *116*, 833–836.
- (41) Schreurs, A. M. M.; Xian, X.; Kroon-Batenburg, L. M. *J. Appl. Crystallogr.* **2010**, *43*, 70–82.
- (42) Herbst-Irmer, R.; Sheldrick, G. M. *Acta Crystallogr., Sect. B: Struct. Sci.* **1998**, *54*, 443–449.
- (43) Beurskens, P. T.; Beurskens, G.; de Gelder, R.; Garcia-Granda, S.; Gould, R. O.; Smits, J. M. M. (2008) *The DIRDIF2008 Program System*; Crystallography Laboratory, University of Nijmegen: The Netherlands.
- (44) Sheldrick, G. M. *Acta Crystallogr.* **2015**, *C71*, 3–8.
- (45) Sheldrick, G. M. (1999) *SADABS: Area-Detector Absorption Correction*, v2.10; Universität Göttingen: Göttingen, Germany.
- (46) Sheldrick, G. M. *Acta Crystallogr., Sect. A: Found. Adv.* **2015**, *71*, 3–8.
- (47) Altomare, A.; Burla, M. C.; Camalli, M.; Cascarano, G. L.; Giacovazzo, C.; Guagliardi, A.; Moliterni, A. G. G.; Polidori, G.; Spagna, R. *J. Appl. Crystallogr.* **1999**, *32*, 115–119.
- (48) Flack, H. D. *Acta Crystallogr., Sect. A: Found. Crystallogr.* **1983**, *39*, 876–881.
- (49) Bruker (2001) *SAINT-Plus*; Bruker AXS Inc.: Madison, WI.
- (50) Sheldrick, G. M. *Acta Crystallogr., Sect. A: Found. Crystallogr.* **2008**, *64*, 112–122.
- (51) The CH<sub>3</sub>CN adduct can be explained by the Lewis acidity of the high-valent trioxo-rhenium species, the use of CH<sub>3</sub>CN for the sample preparation, and the presence of residual Na<sup>+</sup> sources in the ESI-MS setup.